Syntheses and Electronic Spectroscopy of [PtL(L′)][ClO_4] Complexes (HL = 6-Phenyl-2,2′-bipyridine; L′ = Pyridine, 4-Aminopyridine, 2-Aminopyridine, and 2,6-Diaminopyridine)

John H. K. Yip,* Suwarno, and Jagadese J. Vittal

Department of Chemistry, The National University of Singapore, 10 Kent Ridge Crescent, 119260 Singapore

Received November 19, 1999

Four cyclometalated Pt(II) complexes, [PtL(L′)][ClO_4] [HL = 6-phenyl-2,2′-bipyridine; L′ = pyridine (**1**), 4-aminopyridine (**2**), 2-aminopyridine (**3**), 2,6-diaminopyridine (**4**)], were designed and synthesized to probe intramolecular N···Pt interactions. The crystal structures of the compounds show that the pyridine ligands are almost perpendicular to the planes of the molecules. In addition, the pendant NH_2 groups of the 2-aminopyridine and 2,6-diaminopyridine ligands are close to the metal centers in complexes **3** and **4**, with the Pt−N(H_2) distances (3.065(3)−3.107(3) Å) significantly shorter than the sum of the van der Waals radii of Pt and N. These compounds were also studied by electronic spectroscopy. All the complexes display intense intraligand $\pi \rightarrow \pi^*$ transitions at 200−340 nm ($\epsilon = 10^4-10^3$ M^{-1} cm^{-1}) and moderately intense ($\epsilon \sim 10^3$ M^{-1} cm^{-1}) metal (Pt)-to-ligand (π^*) charge-transfer (MLCT) transitions. For **1** and **2**, the MLCT transitions occur at ∼390 nm, but the MLCT transition of **4** is exceptionally low in energy (492 nm). The low-temperature emission spectra of the complexes in frozen EMD glass indicate that $^3\pi\pi^*$ is the emissive excited state for **1** and **2** but the emission of **3** is from a ^{3}MLCT excited state. On the basis of the spectroscopic results, the order of energy of the MLCT excited states is established as **1** ∼ **2** > **3** > **4**. It is proposed that the red shifts of the MLCT transitions in **3** and **4** are due to increased electron-donating abilities of the ancillary pyridine ligands and intramolecular interactions between the orbitals of amine nitrogen lone pairs. Crystal data for the complexes are as follows. **1**: triclinic $P\bar{1}$, $Z = 2$, $a = 8.7917(2)$ Å, $b = 10.6398(3)$ Å, $c = 11.9592(3)$ Å, $\alpha = 107.130(1)°$, $\beta = 92.522(1)°$, $\gamma = 111.509(1)°$. **2**·CH_3CN: triclinic $P\bar{1}$, $Z = 2$, $a = 7.0122(4)$ Å, $b = 12.9653(8)$ Å, $c = 14.0283(9)$ Å, $\alpha = 107.3100(10)°$, $\beta = 102.7640(10)°$, $\gamma = 91.6320(10)°$. **3**·CH_3CN: triclinic $P\bar{1}$, $Z = 2$, $a = 7.6459(1)$ Å, $b = 10.8433(1)$ Å, $c = 14.8722(2)$ Å, $\alpha = 99.383(1)°$, $\beta = 93.494(1)°$, $\gamma = 101.385(1)°$. **4**·CH_3CN: triclinic $P\bar{1}$, $Z = 2$, $a = 7.862(2)$ Å, $b = 10.977(3)$ Å, $c = 14.816(5)$ Å, $\alpha = 99.34(2)°$, $\beta = 92.64(2)°$, $\gamma = 104.11(2)°$.

Introduction

Square planar Pt(II)−polypyridine complexes represent an important class of luminophores in inorganic photochemistry.[1] Brightly colored and strongly emissive, Pt(II)−polypyridine compounds have found applications in areas such as photosensitization,[2] supramolecular photochemistry,[3] and chemical sensing.[4] Polypyridine ligands commonly found in this class of complexes include variously substituted 2,2′-bipyridine (bpy), 1,10-phenanthroline,[2d−f,5] 2,2′:6′,2″-terpyridine (terpy),[6] 6-phenyl-2,2′-bipyridine (HL),[7] and 2,2′:6′,2″:6″,2‴-quaterpyridine (qp).[8] Pt(II)−polypyridine complexes such as $[Pt(qp)]^{2+}$ and $[Pt(bpy)_2]^{2+}$ contain a polypyridine as the only ligand, while, in compounds such as $[Pt(bpy)(X)_2]$[1a,5a−o] and $[Pt(terpy)(X)]^+$ (X = Cl, Br, I, CN, NCS, Me, C_2Ph, OMe),[6a−i] the metal is coordinated to one or two ancillary ligands X in addition to the polypyridine. Many Pt(II)−polypyridine complexes are photoluminescent, and previous spectroscopic investigations showed that the phosphorescence of the complexes arises from one of the following electronic excited states: ligand field (^{3}LF), metal-to-ligand charge transfer (^{3}MLCT), and intraligand ($^3\pi\pi^*$).[1a] Additionally, the natures of the emissive excited states of the complexes are found to be sensitive to the properties of both polypyridine and ancillary ligands. This can be illustrated by

* To whom correspondence should be addressed. E-mail: chmyiphk@nus.edu.sg.

(1) (a) Houlding, V. H.; Miskowski, V. M. *Coord. Chem. Rev.* **1991**, *111*, 145. (b) Pettijohn, C. N.; Jochnowitz, E. B.; Chuong, B.; Nagle, J. K.; Vogler, A. *Coord. Chem. Rev.* **1998**, *171*, 85. (c) Yersin, H.; Humbs, W.; Strasser, J. *Coord. Chem. Rev.* **1997**, *159*, 325. (d) Paw, W.; Cummings, S. D.; Mansour, M. A.; Connick, W. B.; Gieger, D. K.; Eisenberg, R. *Coord. Chem. Rev.* **1998**, *171*, 125.

(2) (a) Chassot, L.; Müller, E.; von Zelewsky, A. *Inorg. Chem.* **1984**, *23*, 4249. (b) Sandrini, D.; Maestri, M.; Balzani, V.; Chassot, L.; von Zelewsky, A. *J. Am. Chem. Soc.* **1987**, *109*, 3107. (c) Vogler, A.; Kunkely, H. *Coord. Chem. Rev.* **1998**, *177*, 81. (d) Wan, K. T.; Che, C. M.; Cho, K. C. *J. Chem. Soc., Dalton Trans.* **1991**, 1077. (e) Che, C. M.; Wan, K. T.; He, L. Y.; Poon, C. K.; Yam, V. W. W. *J. Chem. Soc., Dalton Trans.* **1989**, 2011. (f) Wan, K. T.; Che, C. M. *J. Chem. Soc., Chem. Commun.* **1990**, 140.

(3) (a) Ballardini, R.; Gandolfi, M. T.; Balzani, V.; Kohnke, F. H.; Stoddart, J. F. *Angew. Chem., Int. Ed. Engl.* **1988**, *27*, 692. (b) Ballardini, R.; Gandolfi, M. T.; Prodi, L.; Ciano, M.; Balzani, V.; Kohnke, F. H.; Shahriari-Zavareh; H.; Spencer, N.; Stoddart, J. F. *J. Am. Chem. Soc.* **1989**, *111*, 7072. (c) Tse, M. C.; Cheung, K. K.; Chan, M. C. W.; Che, C. M. *J. Chem. Soc., Chem. Commun.* **1998**, 2295. (d) Chan, C. W.; Lai, T. F.; Che, C. M.; Peng, S. M. *J. Am. Chem. Soc.* **1993**, *115*, 11245.

(4) (a) Liu, H. Q.; Cheung, T. C.; Che, C. M. *J. Chem. Soc., Chem. Commun.* **1990**, 1039. (b) Wu, L. Z.; Cheung, T. C.; Che, C. M.; Cheung, K. K.; Lam, M. H. H. *J. Chem. Soc., Chem. Commun.* **1998**, 1127. (c) Lee, W. W. S.; Wong, K. Y.; Li, X. M. *Anal. Chem.* **1993**, *65*, 255. (d) Cusumano, M.; Di Pietro, M. L.; Giannetto, A. *Inorg. Chem.* **1999**, *38*, 1754. (e) Wong, K. P.; Chan, C. W.; Che, C. M. *Chem.—Eur. J.* **1999**, *10*, 2845. (f) Ma, Y. G.; Cheung, T. C.; Che, C. M.; Shen, J. C. *Thin Solid Films* **1998**, *333*, 224.

10.1021/ic9913482 CCC: $19.00
Published on Web 07/21/2000

the example where the emissions of Pt(II)−polypyridine complexes containing strong-field ligands, such as [Pt(5,5′-Me_2bpy)$(CN)_2$][5g] and [Pt(bpy)(en)]$^{2+}$ (en = ethylenediamine),[5f] arise from intraligand $^3\pi\pi^*$ excited states whereas the emission of the complex [Pt(bpy)Cl_2], which contains the weak-field ligand chloride, originates from a ^{3}LF excited state.[5e,f] The ^{3}MLCT state is the lowest energy excited state for Pt(II) compounds containing either polypyridine ligands that have low-lying π^* orbitals[5e] or strong electron-donating ancillary ligands.[6b,c,e,7a,c] Furthermore, the energy of the MLCT excited state can be tuned by the ancillary ligand, as demonstrated by the red shift of the MLCT transitions of the complexes [Pt(terpy)(X)]$^+$ (X = Cl, Br, I) as X is changed from Cl to the stronger electron-donating Br and I.[6c] Finally, it is known that the ^{3}LLCT state, which is derived from a ligand-to-ligand charge-transfer transition, is the lowest energy excited state for Pt(II)−polypyridine complexes which possess electron-rich thiolates as ancillary ligands.[9]

In addition to those of the polypyridine and ancillary ligands, the spectroscopy and photophysics of Pt(II)−polypyridine complexes are also subject to the influence of intermolecular metal−metal and ligand $\pi-\pi$ interactions. It is well-known that many Pt(II)−polypyridine complexes stack in the solid state via Pt−Pt and/or $\pi-\pi$ interactions, forming dimers or linear chains.[5a−n,6] These weak interactions are also responsible for the dimerization of [Pt(terpy)(Cl)]$^+$ in solution.[6b] Generally, the MLCT transitions of the aggregated Pt complexes in the solid state and solution are red-shifted significantly from those of the monomeric complexes. Besides, intermolecular Pt−Pt interactions also lead to a decrease of MLCT transition energy in binuclear compounds such as [Pt_2(terpy)$_2$(μ-pyrazolate)]$^{3+}$ [10] and [Pt_2L_2(μ-dppm)]$^{2+}$ [7a,d] (dppm = bis(diphenylphosphino)methane). Analogous to the case of the binuclear complex [$Pt_2(P_2O_5H_2)_4$],[4−11] interactions between the $5d_{z^2}$ orbitals of adjacent Pt atoms in these Pt(II)−polypyridine complexes give rise to a bonding dσ and an antibonding dσ^* orbitals and the red-shifted MLCT transition corresponds to the d$\sigma^* \rightarrow \pi^*$ transition.[5d−g,i,6b,c,h,7a,d,10]

Chart 1. Nomenclatures for the Complexes

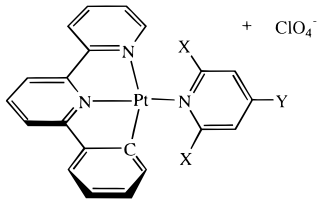

Compound	X	Y
1	H, H	H
2	H, H	NH_2
3	NH_2, H	H
4	NH_2, NH_2	H

In view of the pronounced effect of Pt−Pt interactions on the spectroscopic and photophysical properties of Pt(II)−polypyridine complexes, we were interested to know if the electronic structures of the complexes could be affected by other weak interactions. Especially, we were interested in understanding the effects of intramolecular interactions between lone pairs and metals on the electronic structures. We report herein the syntheses, structures, and electronic spectroscopy of four cyclometalated Pt(II) complexes (Chart 1). Compounds **3** and **4**, which contain the ligands 2-aminopyridine and 2,6-diaminopyridine, were designed to probe the effect of the nitrogen lone pairs on the electronic structures of the complexes, and complexes **1** and **2** were synthesized as reference compounds.

Experimental Section

Materials. Potassium tetrachloroplatinate and lithium perchlorate were obtained from Oxkem and Fluka, respectively. 2-Aminopyridine, 4-aminopyridine, and 2,6-diaminopyridine were purchased from Aldrich and used without further purification. All solvents used in syntheses and spectroscopic measurements were purified according to the literature methods.

Physical Measurements. The UV−vis absorption and low-temperature emission spectra of the complexes were recorded on a Hewlett-Packard HP8452A diode array spectrophotometer and a Perkin-Elmer LS-50D fluorescence spectrophotometer, respectively. All samples used for low-temperature emission spectroscopy were prepared by dissolving the complexes in 5:5:1 mixtures of ethanol/methanol/dimethylformamide (EMD), which formed transparent glasses at 77 K. Sample solutions used for room-temperature emission measurements were degassed with at least three freeze−pump−thaw cycles. The emission

(5) (a) Osborn, R. J.; Rogers, D. J. *J. Chem. Soc., Dalton Trans.* **1974**, 1002. (b) Che, C. M.; He, L. Y.; Poon, C. K.; Mak, T. C. W. *Inorg. Chem*. **1989**, *28*, 3081. (c) Connick, W. B.; Marsh, R. E.; Schaefer, W. P.; Gray, H. B. *Inorg. Chem*. **1997**, *36*, 913. (d) Connick, W. B.; Henling, L. M.; Marsh, R. E.; Gray, H. B. *Inorg. Chem*. **1996**, *35*, 6261. (e) Miskowski, V. M.; Houlding, V. H.; Che, C. M.; Wang, Y. *Inorg. Chem*. **1993**, *32*, 2518. (f) Miskowski, V. M.; Houlding, V. H. *Inorg. Chem*. **1989**, *28*, 1529. (g) Miskowski, V. M.; Houlding, V. H. *Inorg. Chem*. **1991**, *30*, 4446. (h) Crosby, G. A.; Kendrick, K. R. *Coord. Chem. Rev*. **1998**, *171*, 407. (i) Kato, M.; Sasano, K.; Kosuge, C.; Yamazaki, M.; Yano, S.; Kimura, M. *Inorg. Chem*. **1996**, *35*, 116. (j) Bielli, E.; Gidney, P. M.; Gillard, R. D.; Heaton, B. T. *J. Chem. Soc., Dalton Trans.* **1974**, 2133. (k) Coyer, M. J.; Herber, R. H.; Cohen, S. *Inorg. Chim. Acta* **1990**, *175*, 47. (l) Biedermann, J.; Gliemann, G.; Kelment, U.; Ranger, K.-J.; Zabel, M. *Inorg. Chim. Acta* **1990**, *171*, 35. (m) Biedermann, J.; Wallfahrer, M.; Gliemann, G. *J. Lumin.* **1987**, *37*, 323. (n) Weiser-Wallfahrer, M.; Gliemann, G. *Z. Naturforsch.* **1990**, *45B*, 652. (o) Connick, W. B.; Geiger, D.; Eisenberg, R. *Inorg. Chem*. **1999**, *38*, 3264. (p) Chan, C. W.; Cheng, L. K.; Che, C. M. *Coord. Chem. Rev*. **1994**, *132*, 87.

(6) (a) Jennette, K. W.; Gill, J. T.; Sadownick, J. A.; Lippard, S. J. *J. Am. Chem. Soc*. **1976**, *98*, 6159. (b) Bailey, J. A.; Hill, M. G.; Marsh, R. E.; Miskowski, V. M.; Schaefer, W. P.; Gray, H. B. *Inorg. Chem*. **1995**, *34*, 4591. (c) Yip, H. K.; Cheng, L. K.; Cheung, K. K.; Che, C. M. *J. Chem. Soc., Dalton Trans.* **1993**, 2933. (d) Tzeng, B. C.; Fu, W. F.; Che, C. M.; Chao, H. Y.; Cheung, K. K.; Peng, S. M. *J. Chem. Soc., Dalton Trans.* **1999**, 1017. (e) Aldridge, T. K.; Stacy, E. M.; McMillin, D. R. *Inorg. Chem*. **1994**, *33*, 722. (f) Büchner, R.; Field, J. S.; Haines, R. J.; Cunningham, C. T.; McMillin, D. R. *Inorg. Chem*. **1997**, *36*, 3952. (g) Crites, D. K.; Cunningham, C. T.; McMillin, D. R. *Inorg. Chim. Acta* **1998**, *273*, 346. (h) Büchner, R.; Cunningham, C. T.; Field, J. S.; Haines, R. J.; McMillin, D. R.; Summerton, G. C. *J. Chem. Soc., Dalton Trans.* **1999**, 711. (i) Arena, G.; Calogero, G.; Campagna, S.; Scolaro, L. M.; Ricevuto, V.; Romeo, R. *Inorg. Chem*. **1998**, *37*, 2763. (j) Lai, S. W.; Chan, M. C. W.; Cheung, K. K.; Che, C. M. *Inorg. Chem*. **1999**, *38*, 4262.

(7) (a) Cheung, T. C.; Cheung, K. K.; Peng, S. M.; Che, C. M. *J. Chem. Soc., Dalton Trans.* **1996**, 1645. (b) Neve, F.; Crispini, A.; Campagna, S. *Inorg. Chem*. **1997**, *36*, 6150. (c) Lai, S. W.; Chan, M. C. W.; Cheung, K. K.; Che, C. M. *Organometallics* **1999**, *18*, 3327. (d) Lai, S. W.; Chan, M. C. W.; Cheung, T. C.; Peng, S. M.; Che, C. M. *Inorg. Chem*. **1999**, *38*, 4046.

(8) (a) Chan, C. W.; Che, C. M.; Cheng, M. C.; Wang, Y. *Inorg. Chem*. **1992**, *31*. 4874. (b) Constable, E. C.; Elder, S. M.; Hannon, M. J.; Martin, A.; Raithby, P. R.; Tocher, D. A. *J. Chem. Soc., Dalton Trans*. **1996**, 2423.

(9) (a) Zuleta, J. A.; Bevilacqua, J. M.; Proserpio, D. M.; Harvey, P. D.; Eisenberg, R. *Inorg. Chem*. **1992**, *31*, 2396. (b) Cummings, S. D.; Eisenberg, R. *Inorg. Chem*. **1995**, *34*, 2007. (c) Zuleta, J. A.; Chesta, C. A.; Eisenberg, R. *J. Am. Chem. Soc.* **1989**, *111*, 8916. (d) Connick, W. B.; Gray, H. B. *J. Am. Chem. Soc*. **1997**, *119*, 11620.

(10) Bailey, J. A.; Miskowski, V. M.; Gray, H. B. *Inorg. Chem*. **1993**, *32*, 369.

(11) Roundhill, D. M.; Gray, H. B.; Che, C. M. *Acc. Chem. Res*. **1989**, *22*, 55.

Table 1. Crystal Data and Structure Refinement Details for **1**, **2**·CH_3CN, **3**·CH_3CN, and **4**·CH_3CN[a]

	1	**2**·CH_3CN	**3**·CH_3CN	**4**·CH_3CN
empirical formula	$C_{21}H_{16}ClN_3O_4Pt$	$C_{23}H_{20}ClN_5O_4Pt$	$C_{23}H_{20}ClN_5O_4Pt$	$C_{23}H_{21}ClN_6O_4Pt$
fw	604.91	660.98	660.98	676.00
crystal size, mm^3	32 × 13 × 0.04	0.42 × 0.28 × 0.14	0.35 × 0.2 × 0.03	0.33 × 0.25 × 0.13
a, Å	8.7917(2)	7.0122(4)	7.6459(1)	7.862(2)
b, Å	10.6398(3)	12.9653(8)	10.8433(1)	10.977(3)
c, Å	11.9592(3)	14.0283(9)	14.8722(2)	14.816(5)
α, deg	107.130(1)	107.3100(10)	99.383(1)	99.34(2)
β, deg	92.522(1)	102.7640(10)	93.494(1)	92.64(2)
γ, deg	111.509(1)	91.6320(10)	101.385(1)	104.11(2)
V, $Å^3$	979.97(4)	1181.44(12)	1187.03(2)	1218.8(6)
ρ_{calcd}, g cm^{-3}	2.050	1.858	1.849	1.842
GOF on F^2	1.016	1.034	0.970	1.165
μ, cm^{-1}	7.330	6.091	6.0631	5.908
F(000)	580	640	640	656
R1[b] [$I \geq 2\sigma(I)$]	0.0362	0.0533	0.0527	0.0487
wR2[c] [$I \geq 2\sigma(I)$]	0.0923	0.1259	0.1181	0.1180

[a] For all compounds: triclinic crystal system, space group $P\bar{1}$; $Z = 2$; $\lambda = 0.710\ 73$ Å. [b] $R1 = \sum||F_o| - |F_c||/\sum|F_o|$. [c] $wR2 = [\sum w(F_o^2 - F_c^2)/(\sum wF_o^4]^{1/2}$.

quantum yields were measured with $[Ru(bipy)_3][PF_6]_2$ in degassed acetonitrile as the standard. ^1H NMR spectra were recorded at 25 °C on a Bruker ACF 300 spectrometer. Elemental analyses of the complexes were carried out in the microanalytical laboratory of the Department of Chemistry at the National University of Singapore. Emission lifetime measurements were performed with a Quanta Ray DCR-3 pulsed Nd:YAG laser system (pulse output 355 nm, 8 ns). The emission signals were detected by a Hamamatsu R928 photomultiplier tube and recorded on a Tektronix model 2430 digital oscilloscope.

Syntheses of Metal Complexes 1−4. The compounds 6-phenyl-2,2′-bipyridine[12] (HL) and [PtL(Cl)][13] were synthesized according to the reported methods. The same procedure was adopted for the syntheses of the four complexes [PtL(L′)][ClO_4] [L = pyridine (**1**), 4-aminopyridine (**2**), 2-aminopyridine (**3**), 2,6-aminopyridine (**4**)]: An excess amount of ligand L′ (∼0.2 g) was added to a suspension of [PtL(Cl)] (0.5 g, 1.1 mmol) in methanol (30 mL), and the mixture was refluxed until the solution became clear. The solution was filtered and excess $LiCO_4$ was added to precipitate the product. The solid collected after filtration was washed with excess methanol, and the product was purified by slow diffusion of diethyl ether into an acetonitrile solution. **1**: yield 85%. Anal. Calcd for $C_{21}H_{16}N_3PtClO_4$: C, 41.7; H, 2.6; N, 6.9. Found: C, 41.2; H, 2.7; N, 6.9. ^1H NMR (CD_3CN, 300 MHz; δ): 7.05−7.23 (m, 3H), 7.37−7.45 (m, 1H), 7.48−7.55 (m, 1H), 7.59−7.65 (m, 1H), 7.68−7.82 (m, 3H), 7.89−8.12 (m, 3H), 8.15−8.26 (m, 2H), 8.65 (m, 1H), 8.98 (m, 1H). **2**·CH_3CN yield: 75%. Anal. Calcd for $C_{23}H_{20}N_5PtClO_4$: C, 41.8; H, 3.0; N, 10.6. Found: C, 41.6; H, 2.9; N, 10.3. ^1H NMR (CD_3CN, 300 MHz; δ): 5.76 (b, 2H), 6.59 (m, 1H), 6.79 (d, 2H), 7.14 (m, 2H), 7.57 (m, 1H), 7.69 (m, 1H), 7.80 (m, 1H), 7.92 (m, 1H), 8.05 (m, 2H), 8.13 (m, 1H), 8.23 (d, 1H), 8.26 (m, 2H). **3**·CH_3CN: yield 64%. Anal. Calcd for $C_{23}H_{20}N_5PtClO_4$: C, 41.8; H, 3.0; N, 10.6. Found: C, 41.5; H, 3.0; N, 10.4. ^1H NMR (CD_3CN, 300 MHz; δ): 6.18 (b, 2H), 6.51 (dd, 1H), 6.55−6.62 (m, 1H), 6.84 (t, 1H), 6.96 (d, 1H), 7.10−7.17 (m, 2H), 7.55−7.85 (m, 4H), 7.88−7.96 (m, 1H), 8.05−8.11 (m, 2H), 8.22−8.26 (m, 2H). **4**·CH_3CN: yield 48%. Anal. Calcd for $C_{23}H_{21}N_6PtClO_4$: C, 40.9; H, 3.2; N, 12.4. Found: C, 41.0; H, 3.2; N, 12.6. ^1H NMR (CD_3CN, 300 MHz; δ): 5.95 (b, 4H), 6.11−6.18 (m, 2H), 6.48−6.66 (m, 1H), 7.08−7.18 (m, 2H), 7.47 (t, 1H), 7.58 (m, 1H), 7.64 (m, 1H), 7.85 (m, 1H), 7.96 (m, 1H), 8.10 (t, 2H), 8.21−8.28 (m, 2H).

X-ray Crystallography. The diffraction experiments were carried out on a Bruker AXS SMART CCD three-circle diffractometer with an Mo Kα sealed tube at 23 °C. The softwares used were SMART[1] for collecting frames of data, indexing reflections, and determination of lattice parameters; SAINT[14] for integration of intensities of reflections and scaling; SADABS[15] for empirical absorption corrections; and SHELXTL[16] for space group determinations and structure solutions and least-squares refinements on $|F|^2$. The crystals were mounted at the end of glass fibers and used for the diffraction experiments. A brief summary of crystal data and experimental details is given in Table 1.

Compound 1. A total of 9213 reflections were collected in the 2θ range 2.18−29.40° ($-12 \leq h \leq 11$, $-13 \leq k \leq 14$, $-15 \leq l \leq 15$), of which 4743 ($R_{int} = 0.0305$) were independent. The oxygen atoms of the perchlorate anion were found to be disordered. Two orientations of oxygen atoms were included in the model with occupancies of 0.75 and 0.25. Common isotropic thermal parameters were refined for each groups, and anisotropic thermal parameters were refined for the remainder of the non-hydrogen atoms. The hydrogen atoms were placed in their ideal positions. An extinction coefficient was refined to 0.0009(5). The electron densities fluctuated between +1.283 and −1.178 e $Å^{-3}$ in the final Fourier difference map.

Compound 2·CH_3CN. The number of reflections collected in the 2θ range 2.61−29.36° ($-9 \leq h \leq 9$, $-17 \leq k \leq 16$, $0 \leq l \leq 9$) was 9040, of which 5630 ($R_{int} = 0.0273$) were independent. The perchlorate anion was disordered and was modeled with three sets of sites for the O atoms; their occupancies were refined but restrained to sum to unity. All Cl−O bond lengths and O−Cl−O bond angles (within each set) were restrained to be the same, and all O atoms were given a fixed isotropic parameter of 0.15 $Å^2$. Common isotropic thermal parameters were refined for the oxygen atoms of each model. An acetonitrile solvate was found in the Fourier difference map. All the non-hydrogen atoms excluding the disordered oxygen atoms were refined anisotropically, and all hydrogen atoms were included in their calculated positions. In the final least-squares cycles, the leftover electron densities were in the range +1.526 to −1.176 e $Å^{-3}$.

Compound 3·CH_3CN. The number of reflections collected in the 2θ range 2.18−29.2° ($-10 \leq h \leq 10$, $-14 \leq k \leq 14$, $-19 \leq l \leq 19$) was 11 055, of which 5676 ($R_{int} = 0.0500$) were independent. The oxygen atoms of the perchlorate anion were found to be disordered. Three disorder models with occupancies of 0.4, 0.4, and 0.2 were included in the least-squares cycles. Common isotropic thermal parameters were refined for the oxygen atoms of each model. An acetonitrile solvate was found in the Fourier difference map. All the non-hydrogen atoms excluding the disordered oxygen atoms were refined anisotropically, and all hydrogen atoms were included in their calculated positions. In the final least-squares cycles, the leftover electron densities were in the range +1.911 to −2.405 e $Å^{-3}$.

(12) Dietrich-Cornioley, C. O.; Marnot, P. A.; Sauvage, J. P. *Tetrahedron Lett*. **1982**, *23*, 5291.
(13) Constable, E. C.; Henney, R. P. G.; Leese, T. A.; Tocher, D. A. *J. Chem. Soc., Chem. Commun*. **1990**, 513.
(14) *SMART & SAINT Software Reference Manual*, Version 4.0; Siemens Energy & Automation, Inc.: Madison, WI, 1996.
(15) Sheldrick, G. M. *SADABS: A software for empirical absorption corrections*; University of Göttingen: Göttingen, Germany, 1996.
(16) *SHELXTL Reference Manual*, Version 5.03; Siemens Energy & Automation, Inc.: Madison, WI, 1996.

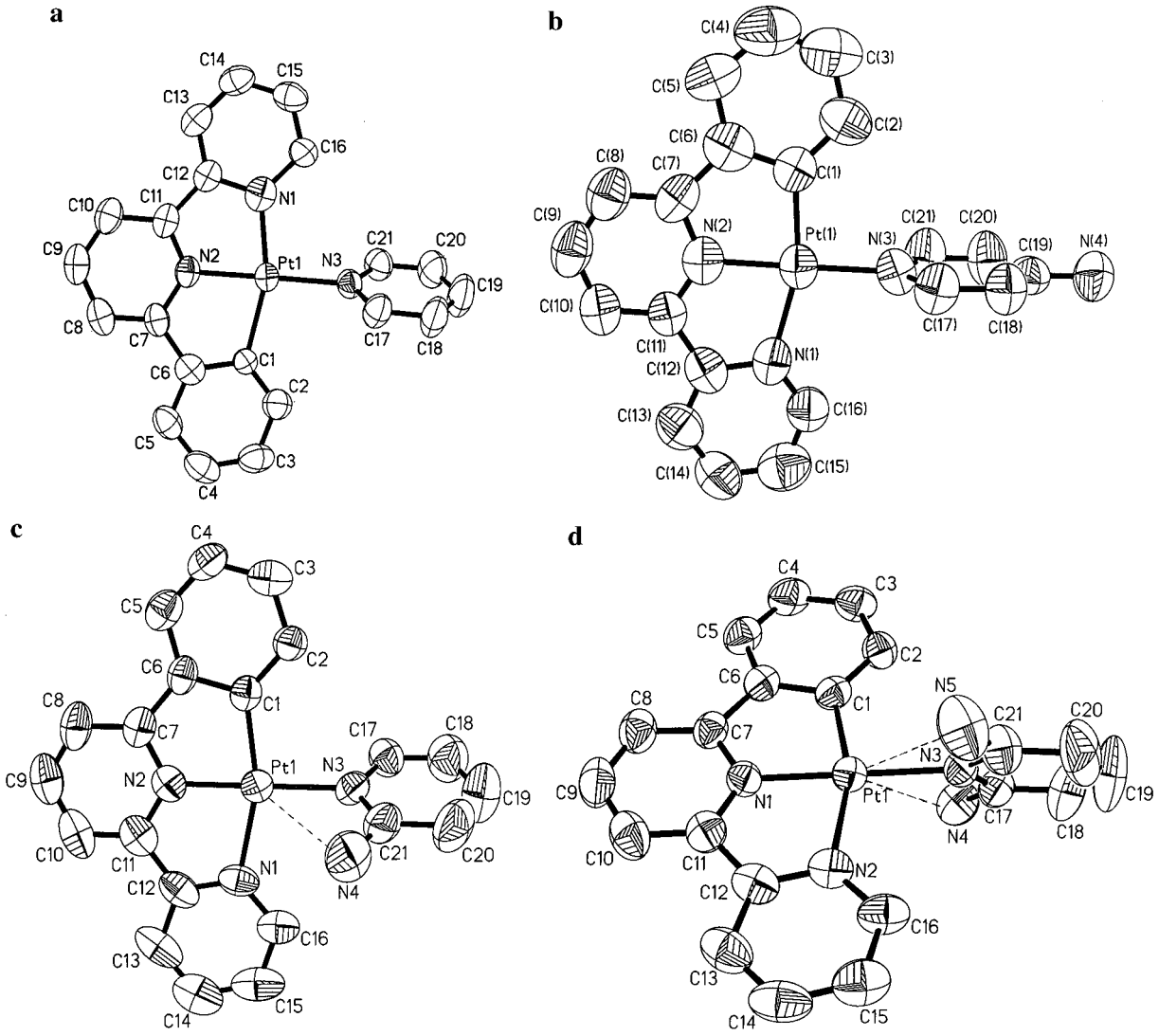

Figure 1. Molecular structures of the cations in (a) **1**, (b) **2**·CH_3CN, (c) **3**·CH_3CN, and (d) **4**·CH_3CN (ORTEP drawings with 50% probability of ellipsoids).

Compound 4·CH_3CN. A total of 7257 reflections were collected in the 2θ range 2.59−29.21° ($-10 \le h \le 10$, $-12 \le k \le 12$, $-19 \le l \le 20$), of which 5210 ($R_{int} = 0.0262$) were independent. The oxygen atoms of the perchlorate anion were found to be disordered. Four independent orientations of the oxygen atoms were resolved and included in the model with occupancies of 0.4, 0.3, 0.2, and 0.1. Common isotropic thermal parameters were refined for each model, and isotropic thermal parameters were refined for the remainder of the non-carbon atoms. An acetonitrile solvate was found in the crystal lattice. In the final Fourier difference map, the electron densities fluctuated in the range +1.583 to −2.276 e $Å^{-3}$.

Results and Discussion

Crystal Structures. The X-ray crystal structures of the cations of **1**−**4** are shown in Figure 1, and selected bond lengths and angles are listed in Table 2. As expected for mononuclear d^8 Pt(II) complexes, the Pt atoms in the four complexes are all four-coordinate, showing distorted square planar geometries. The cyclometalated PtL units are essentially planar. Metal−ligand bond lengths and angles in the four PtL moieties are similar and are close to those observed in related complexes such as $[PtL(CH_3CN)]^+$ [13] and $[PtL(PPh_3)]^+$.[7a] The Pt−N(pyridine) bond distances in **1** (2.029(6) Å) and **2** (2.032(8) Å) are slightly shorter than those in **3** (Pt(1)−N(3) = 2.049(7) Å) and **4** (Pt(1)−N(3) = 2.052(7) Å), but all of them are shorter than the reported Pt−N bond lengths in *trans*-$[Pt(pyridine)_2Cl_2]$ (Pt−N = 2.085 Å).[17] A common feature of the four complexes is the near-perpendicular orientation of the ancillary pyridine ligands with respect to the plane of the cyclometalated PtL unit. The dihedral angles, defined by N(2)−Pt(1)−N(3)−C(17), are 118.3, 92, 114.5, and 112° for **1**−**4**, respectively. Probably, this orientation of the pyridine ligands is adopted to relieve the steric repulsion between the cyclometalated ligand and the NH_2 groups or hydrogen atoms at the 2- and 6-positions of the pyridine ligands. It is noted that, for complexes **2**−**4**, the C−N bonds between the amine substituents and the pyridine rings are shorter than a normal C−N(H_2) single bond (∼1.44 Å), indicating that there is a delocalization of the lone pair electrons of the amine nitrogens into the pyridine rings and the C−N(H_2) bonds possess some double-bond character. Because of the perpendicular orientation of the pyridine rings, the pendant NH_2 groups in 2-aminopyridine and 2,6-diaminopyridine are located above the Pt centers in **3** and **4**. The Pt−N(H_2) distances in **3** (3.107(3) Å) and **4** (3.065(3), 3.083(3) Å) are longer than Pt−N covalent bonds but are significantly shorter than the sum of the van der Waals radii of Pt and N, which is known to be around 3.25−3.35 Å.[18]

(17) Forsellini, E.; Bombieri, G.; Crociani, B.; Boschi, T. *J. Chem. Soc., Chem. Commun.* **1970**, 1203.

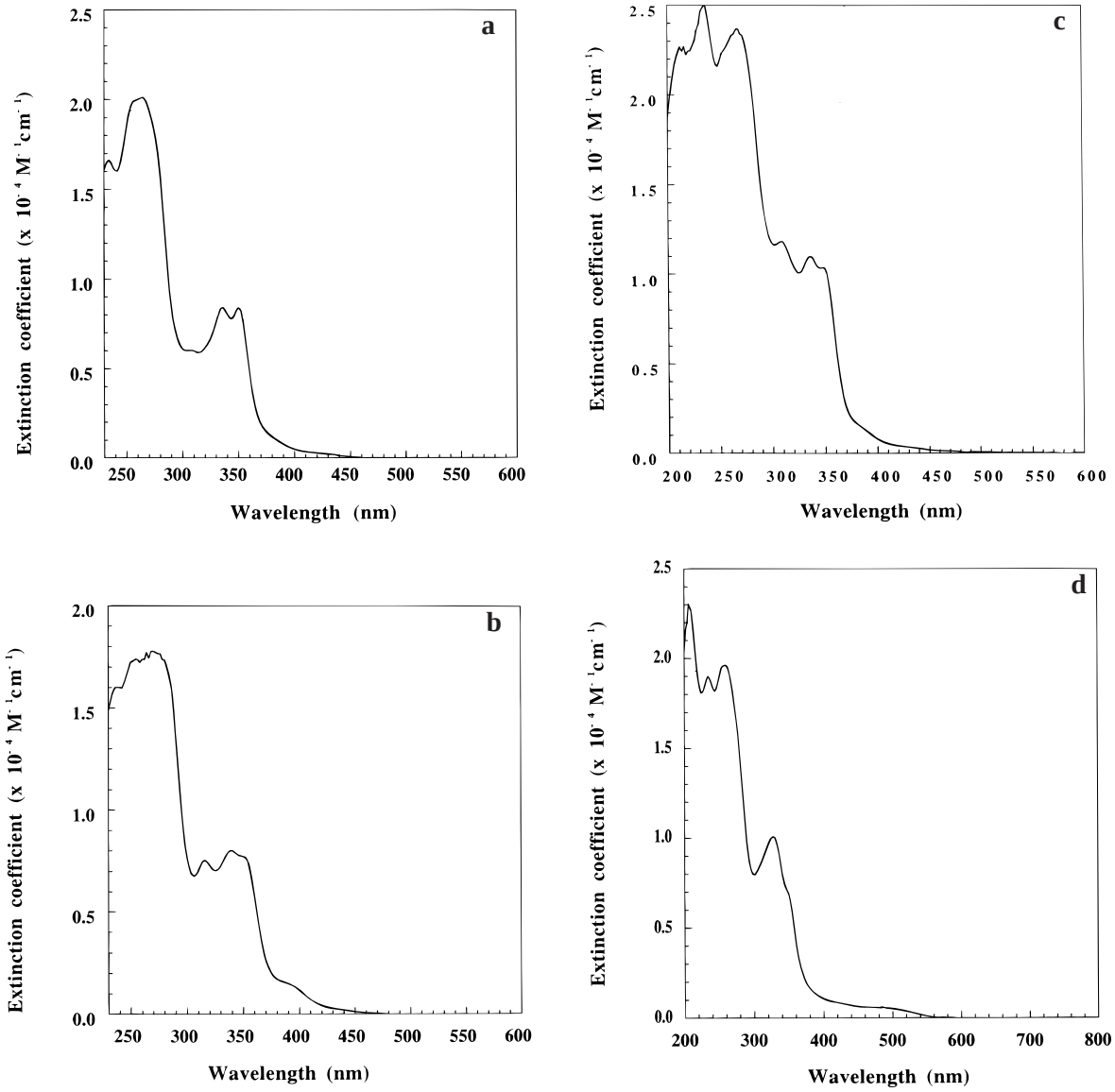

Figure 2. UV−vis absorption spectra recorded in acetonitrile at 298 K: (a) **1**; (b) **2**; (c) **3**; (d) **4**.

Absorption Spectroscopy. Figure 2 shows the solution absorption spectra of **1**−**4**. Previous spectroscopic studies showed that Pt(II)−polypyridine complexes usually exhibit three types of electronic transitions: ligand field (d−d), intraligand $\pi-\pi^*$, and metal-to-ligand charge-transfer (MLCT) transitions.[1a] Given the strong-field nature of the ligands in **1**−**4**, the d−d transitions of the complexes are expected to lie in the high-energy region (<300 nm) and would be masked by the intense $\pi-\pi^*$ transitions.[19] Accordingly, only the $\pi-\pi^*$ and the MLCT transitions need to be considered in assigning the low-energy absorption features of the compounds.

All of the spectra of the complexes show intense absorptions in the range 220−340 nm ($\epsilon = 10^4-10^3$ M^{-1} cm^{-1}), whose energies and shapes are typical for intraligand (L) $^1\pi \rightarrow \pi^*$ transitions. Similar absorptions have been found in the solution spectra of the related compounds [PtL(Cl)] and [PtL(PPh_3)]-[ClO_4].[7a] In addition to the $^1\pi \rightarrow \pi^*$ absorptions, the solution spectrum of **1** also displays a shoulder around 380 nm (ϵ = 1207 M^{-1} cm^{-1}), which is assigned to a ^{1}MLCT (5d(Pt) → p*(L)) transition. ^{1}MLCT absorptions showing similar extinction coefficients have been located in the electronic spectra of related Pt(II)−polypyridine complexes such as [PtL(Cl)] (400−445 nm; $\epsilon = 1550-1020$ M^{-1} cm^{-1})[7a] and [Pt(terpy)(Cl)]$^+$ (372 nm; $\epsilon = 1300$ M^{-1} cm^{-1}).[6b,c,e] The spectrum also shows a weak absorption in the 400−450 nm range ($\epsilon \sim 300$ M^{-1} cm^{-1}), which is attributable to the forbidden ^{3}MLCT and/or $^3\pi\pi^*$ transitions. The spectrum of **2** shows a more distinct absorption band at 390 nm ($\epsilon_{max} = 1527$ M^{-1} cm^{-1}), which tails off toward ~450 nm. Since the 390 nm absorption band resembles the 380 nm shoulder in the spectrum of **1** in both energy and extinction coefficient, it is also assigned to the Pt → π^* ^{1}MLCT transition. The weak absorption at ~430 nm ($\epsilon = 318$ M^{-1} cm^{-1}) could be due to both ^{3}MLCT and $^3\pi\pi^*$ transitions. The absorption spectrum of **3** also exhibits an MLCT absorption band in the 380−450 nm range ($\epsilon_{390nm} = 1196$ M^{-1} cm^{-1}). In addition, the spectrum shows absorptions around 500 nm ($\epsilon \sim 50$ M^{-1} cm^{-1}). The absorption band could be due to a ^{3}MLCT transition, as no such low-energy absorption is observed in the spectra of **1** and **2**. This is further supported by a low-temperature emission study, which shows that the lowest energy excited state of **3** is

(18) Huheey, J. E. *Inorganic Chemistry: Principles of Structures and Reactivity*, 2nd ed.; Harper & Row: New York, 1978; p 232.
(19) The energies of the ligand field transitions of **1**−**4** are expected to be similar to those of Pt(II) tetraamine complexes (<285 nm) (Mason, W. R.; Gray, H. B. *J. Am. Chem. Soc*. **1968**, *90*, 5721).

Table 2. Selected Bond Lengths (Å) and Angles (deg) for **1**,**2**·CH_3CN, **3**·CH_3CN, and **4**·CH_3CN

Complex **1**			
Pt(1)−N(1)	2.092(6)	Pt(1)−N(3)	2.029(6)
Pt(1)−N(2)	1.946(6)	Pt(1)−C(1)	2.004(7)
N(1)−Pt(1)−N(2)	81.1(3)	N(1)−Pt(1)−N(3)	99.4(3)
N(2)−Pt(1)−C(1)	80.0(2)		
Complex **2**·CH_3CN			
Pt(1)−N(1)	2.087(8)	Pt(1)−C(1)	1.999(10)
Pt(1)−N(2)	1.962(7)	C−N(4)	1.349(12)
Pt(1)−N(3)	2.032(8)		
N(1)−Pt(1)−N(2)	79.5(3)	N(1)−Pt(1)−N(3)	101.2(3)
N(2)−Pt(1)−C(1)	82.8(4)		
Complex **3**·CH_3CH			
Pt(1)−N(1)	2.123(7)	Pt(1)−C(1)	1.995(8)
Pt(1)−N(2)	1.938(7)	C(21)−N(4)	1.291(13)
Pt(1)−N(3)	2.052(7)	Pt(1)···N(4)	3.107(3)
N(1)−Pt(1)−N(2)	79.6(3)	N(3)−Pt(1)−N(1)	100.6(3)
N(2)−Pt(1)−C(1)	82.3(3)		
Complex **4**·CH_3CN			
Pt(1)−N(1)	2.112(7)	C(17)−N(4)	1.346(12)
Pt(1)−N(2)	1.952(7)	C(21)−N(5)	1.333(14)
Pt(1)−N(3)	2.049(7)	Pt(1)···N(4)	3.083(3)
Pt(1)−C(1)	2.005(8)	Pt(1)···N(5)	3.065(3)
N(1)−Pt(1)−N(2)	79.7(3)	N(2)−Pt−N(3)	99.4(4)
N(2)−Pt(1)−C(1)	82.0(3)		

^{3}MLCT in nature (vide infra). On the whole, the absorption spectrum of **4** is similar to those of **1**−**3** in the range 200−340 nm, showing intense $^1\pi \rightarrow \pi^*$ transitions. However, the spectrum shows striking differences in the region beyond 400 nm. Unlike the other three compounds, which have no or very weak absorptions beyond 500 nm, **4** displays a moderately intense absorption band peaking at 492 nm (ϵ_{max} = 748 M^{-1} cm^{-1}). The absorption obeys Beer's law in the concentration range 10^{-5}−10^{-3} M, indicating there is no dimerization of complex **4** in solution and the absorptions are from monomeric complexes. On the basis of its extinction coefficient, which is very close to those of ^{1}MLCT absorption bands of other Pt(II)−polypyridine complexes, the absorption band at 492 nm is assigned to the ^{1}MLCT transition. Unfortunately, because of the poor solubility of the complex in other organic solvents, the solvatochromism of the absorption band cannot be demonstrated.

Emission Spectroscopy. The emission spectra (EMD glass at 77 K) and photophysical data of **1**−**3** are shown in Figure 3 and Table 3, respectively. Emissions of **1** and **2** are almost identical in both energy and shape. Both emissions are highly structured (λ_{max} = 502 nm), showing a vibrational progression of ∼1300 cm^{-1}, attributable to the averaged frequency of the C═N and C═C stretches of L in the excited state.[20] The emissions are close in energy and shape to the $^3\pi\pi^*$ emission (λ_{max} = 484 nm) of the cyclometalated gold(III) complex $[Au^{III}L(PPh_3)][ClO_4]$ (H_2L = 2,6-diphenylpyridine).[21] Similarly structured emissions have also been observed in the spectra of other Pt(II)−polypyridine complexes,[5f,i,6f,i] and the emissive

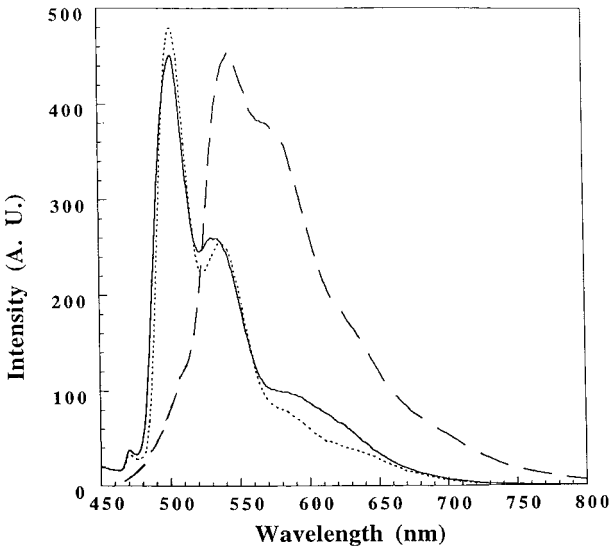

Figure 3. Emission spectra of **1** (—), **2** (···), and **3** (− −) in EMD glass at 77 K. Excitation wavelength = 390 nm.

Table 3. Photophysical Properties of Complexes **1**−**3**[a]

complex	τ; λ_{max}; ϕ_{em}[b]	τ; λ_{max}[c]
1	0.18; 494; 0.05	14.1; 490
2	0.10; 495; 0.06	10.1; 490
3	0.31; 531; 0.01	13.4; 520

[a] τ = lifetime in ms; λ_{max} = emission maximum in nm; ϕ_{em} = emission quantum yield. [b] Quantities were measured at room temperature in a degassed acetonitrile solution; excitation wavelength = 390 nm. [c] Quantities were measured at 77 K in a frozen glass of ethanol/methanol/dimethylformamide (5:5:1); excitation wavelength = 390 nm.

states are usually assigned to the ligand-centered $^3\pi\pi^*$ excited state. The similar energies and shapes of the emission bands of **1** and **2** support the $^3\pi\pi^*$ assignment, as one would expect the energy of the ligand-centered $^3\pi\pi^*$ excited state not to be affected by the ancillary ligand. The assignment is also in accord with the studies of Miskowski and Houlding, which showed that the lowest energy (emissive) excited states of Pt(II)−polypyridine complexes containing strong-field ligands are intraligand $^3\pi\pi^*$ in nature.[1a,5f] The emission of **3** is remarkably different from $^3\pi\pi^*$ emissions of **1** and **2** (Figure 3b). The emission band of **3** is lower in energy (λ_{max} = 540 nm) than the $^3\pi\pi^*$ emissions of **1** and **2**, and its vibronic structures are not well-resolved, showing a spacing of ∼1400 cm^{-1}. The shape and energy of the emission are typical for the ^{3}MLCT emissions exhibited by the related compounds [PtL(Cl)][7a] and the carbene complex $\{PtL[C(NHCH_3)(NHPh)]\}^+$,[7c] which contain strongly electron-donating ancillary ligands. Notably, excitation at the $^1\pi-\pi^*$ absorption band of the complex (340 nm) leads to the same ^{3}MLCT emission, suggesting the energy of the ^{3}MLCT excited state is lower than that of the $^3\pi\pi^*$ state and the internal conversion from the $^3\pi\pi^*$ state to ^{3}MLCT state is very facile. It is found that the room-temperature emission spectra of complexes **1**−**3** in degassed acetonitrile solutions are almost identical to the corresponding 77 K spectra. Unlike the other compounds, **4** is not emissive, even at 77 K. The excited state of **4** may undergo intramolecular electron transfer with the reducing 2,6-diaminopyridine ligands, which would render the complex nonemissive.

Origins of the Red Shift. The most remarkable spectroscopic feature of the present compounds is the dramatic red shift of the MLCT transitions exhibited by **3** and **4**. The emission studies showed that the ^{3}MLCT state of **3** is lower in energy than those

(20) In ref 7d, Che et al. reported the solution emission spectra of **1** at room temperature. The emission was found to be red-shifted at high complex concentration. In our study of the emission spectrum of **1** in frozen EMD glass at 77 K, we also observed an additional emission band at ∼650 nm at high concentration (>10^{-4} M). However, the $^3\pi\pi^*$ emission band is the only observable emission when the concentration of the complex is low (<10^{-5} M).

(21) Wong, K. H.; Cheung, K. K.; Chan, M. C. W.; Che, C. M. *Organometallics* **1998**, *17*, 3505.

of **1** and **2**. Unfortunately, the ^{3}MLCT emission of **4** cannot be detected. Nevertheless, the absorption spectrum of **4** clearly shows that the MLCT transitions of the complex are red-shifted. It is known that the energy of an MLCT excited state is dependent on the σ-donating ability of the ancillary ligand. Usually a strong σ-donating ligand would destabilize the Pt orbitals, leading to a decrease in the energy gap between the metal orbitals and the π^* orbitals and consequently a red shift of the MLCT transition.[6c] For instance, the reported MLCT transition of [PtL(Cl)] (400−445 nm; ϵ = 1550−1020 M^{-1} cm^{-1})[7a] is lower in energy than those of **1** and **2**, in accord with the fact that chloride is a stronger σ donor than pyridines. Because of the lone-pair delocalization, the 2-aminopyridine and 2,6-diaminopyridine ligands in **3** and **4** are stronger electron donors, and accordingly the MLCT transitions of the complexes are expected to be lower in energy. However, the MLCT excited state of **3** is lower than that of **2**, despite the very similar electron-donating abilities of the ligands 2-aminopyridine and 4-aminopyridine in the two complexes. This suggests the red shift of MLCT transitions in **3** (and **4**) is not solely due to the increased electron-donating ability of the ancillary ligand. We believe that *intramolecular* N···Pt interactions between the amine nitrogen lone-pair orbitals and a dπ orbital of the Pt center red shift may contribute to the red shifts of the MLCT transitions in **3** and **4**. The crystal structures of **3** and **4** show that the pendant NH_2 groups in 2-aminopyridine and 2,6-diaminopyridine are close to the Pt centers. The Pt−N(H_2) distances (3.065(3)−3.107(3) Å) are significantly shorter than the sum of van der Waals radii of Pt and N (3.25−3.35 Å),[18] suggesting orbital interactions between the nitrogen and platinum atoms are possible. These orbital interactions are expected to destabilize the metal orbitals (i.e., dπ orbitals), leading to a lowering of the MLCT transition energies.

Interactions between Pt(II) centers and the pendant amine lone pairs have been postulated to be responsible for the facile oxidation of some Pt(II) complexes that contain triaza ligands.[22] For example, it was found that a mixture of [Pt(bpy)($Cl)_2$] and tach (*cis*,*cis*-1,3,5-triaminocyclohexane) can be oxidized to [Pt^{IV}(tach-H_2)(bpy)(H_2O)]Cl_2 (tach-H_2 = tach dianion) under very mild conditions.[22a] An intermediate [Pt(bpy)(tach)]$^{2+}$ was proposed, in which an uncoordinated NH_2 group of tach interacts with the filled $5d_{z^2}$ orbital of the Pt(II) center. It was suggested that the removal of electrons from the Pt center is facilitated by the N···Pt interaction. Similarly, the enhanced oxidizability of the complex [Pt(1,4,7-triazacyclononane)$_2$]$^{2+}$ was explained by the interactions of the Pt center with the dangling amine lone pairs.[22b] We also noted that orbital interactions between metal centers and pendant lone pairs, similar to the N···Pt interactions proposed in this work, were described by Cotton et al. in their recent study[23] of the binuclear compound [Cr_2(DPhIP)$_4$] (DPhIP = 2,6-bis(phenylimino)piperidine anion). The complex was found to have an exceptionally long Cr−Cr bond (2.265(1) Å) in comparison with other binuclear chromium compounds such as [Cr_2(PhIP)$_4$] (PhIP = 2-(phenylimino)piperidine anion; Cr−Cr = 1.858(1) Å). The ligand DPhIP contains a pendant imine group, and the lengthening of the Cr−Cr bond in [Cr_2(DPhIP)$_4$] was attributed to axial interactions between the imino nitrogen lone-pair orbitals and the dπ^* orbitals of the Cr−Cr quadruple bond, which lead to transfer of electron density from the lone pairs to the dπ^* orbitals.

Concluding Remarks

In this study we reported the crystal structures of four cyclometalated Pt(II) complexes that contain substituted pyridines as ancillary ligands. The most intriguing spectroscopic feature of these complexes is the red shift of the MLCT transitions exhibited by **3** and **4**. The photophysical and spectroscopic properties of the cyclometalated complexes [PtL(L′)][ClO_4] are found to be sensitive to the immediate environment of the metal center. The results of emission and absorption spectroscopic studies show the energies of the MLCT excited states of the complexes to be in the order **1** ∼ **2** > **3** > **4**. The red shift of the MLCT transitions of **3** and **4** could be due to the increased electron-donating abilities of the ancillary ligands and intramolecular N···Pt interactions between the lone-pair orbitals of the dangling NH_2 groups and the Pt $5d_{xz}$ orbitals. Finally, the fact that the electronic structures of the Pt(II) complexes can be significantly affected by the N···Pt interactions suggest that these interactions might be useful in tuning the photochemical and photophysical properties of Pt(II) complexes.

Acknowledgment. The authors are grateful to the National University of Singapore for financial support. J.H.K.Y. thanks Dr. Leong Weng Kee for solving the X-ray structure of compound **2** and Prof C. M. Che and Dr. K. C. Chan at The University of Hong Kong for assistance with the emission lifetime measurements. Mr. Chen Min is thanked for his assistance with the absorption measurements.

Supporting Information Available: Tables of crystallographic data collection parameters, atomic coordinates, thermal parameters, and complete bond lengths and bond angles for **1**, **2**·CH_3CN, **3**·CH_3CN, and **4**·CH_3CN. This material is available free of charge via the Internet at http://pubs.acs.org.

IC9913482

(22) (a) Sarneski, J. E.; McPhail, A. T.; Onan, K. D.; Erickson, L. E.; Reilley, C. N. *J. Am. Chem. Soc.* **1977**, *99*, 7376. (b) Wieghardt, K.; Köppen, M.; Swiridoff, W.; Weiss, J. *J. Chem. Soc., Dalton Trans.* **1983**, 1869. (c) Davies, M. S.; Hambley, T. W. *Inorg. Chem.* **1998**, *37*, 5408.

(23) Cotton, F. A.; Daniels, L. M.; Murillo, C. A.; Pascual, I.; Zhou, H.-C. *J. Am. Chem. Soc.* **1999**, *121*, 6856.